Right but not left hemispheric discrimination of faces in infancy

Parvaneh Adibpour, Jessica Dubois, Ghislaine Dehaene-Lambertz

Right but not left hemispheric discrimination of faces in infancy

Parvaneh Adibpour MSc, Jessica Dubois PhD, Ghislaine Dehaene-Lambertz MD-PhD*

Affiliations:

INSERM, UMR992; CEA, NeuroSpin Center; University Paris Saclay, Gif-sur-Yvette, France

# of tables: 2
# of figures: 6
# of pages (including abstract, text, references): 24
# of words in abstract: 150

Corresponding address
Ghislaine Dehaene-Lambertz
CEA/SAC/DRF/I2BM/NeuroSpin/Cognitive Neuroimaging Unit U992
Bât 145, point courrier 156
91191 Gif-sur-Yvette, France
Email: gdehaene@gmail.com
Phone: +33 1 69 08 81 72
Fax: +33 1 69 08 79 73

Abstract

The ontogeny of the human brain functional asymmetries is poorly understood. Are they a consequence of differential development based on competition mechanisms, or are they constitutive of the human brain architecture from the start? Using structural MRI and a face discrimination EEG paradigm with lateralized presentation of faces, we studied face perception in infants over the first postnatal semester. We showed that the corpus callosum is sufficiently mature to transfer visual information across hemispheres, but the inter-hemispheric transfer time of early visual responses is modulated by callosal fibers myelination. We also revealed that only the right hemisphere shows evidence for face discrimination when presented in the left visual-hemifield. This capability improved throughout the first semester with no evidence of discrimination in the left hemisphere. Face processing lateralization is thus a characteristic of the infant's extra-striate visual cortex, highlighting the differential left-right organization of the human brain already established in infanthood.

Keywords: Face perception, Visual system, Infancy, Brain Development, Hemispheric Lateralization, Myelination, EEG, Diffusion MRI

The adult human brain is parcellated into multiple functional regions which are remarkably similar across individuals despite differences in cultural, linguistic, or socio-economic background. Even for culturally learned skills such as reading, similarly-localized activations are observed across writing systems and ages of acquisition[1] revealing the weight of structural constraints on functional architecture. Despite a growing body of evidence on the existence of specialized functional modules in the adult brain, the developmental course of such functional specialization is still poorly understood. Hemispheric functional asymmetries represent a radical example of functional specialization since *a-priori* similar cortical areas end up with different functional specificities.

Here, we aimed to understand the origin of the right-hemispheric advantage for face processing. Two main hypotheses can be proposed. First, structural differences between hemispheres result in a better efficiency of the right hemisphere to process faces from the start. These structural differences might be determined early on during gestation based on cortical "protomaps"[2]. They might also be driven or amplified by maturational asymmetries in gray matter or white matter pathways, which would give rise to a transitory advantage in one hemisphere when infants are exposed to frequent and expected stimuli such as speech and faces[3,4]. In line with this first hypothesis, asymmetries in cortical maturation[5] and in bundle myelination[6,7] have already been reported in the language network during the first semester after birth. The second hypothesis postulates that both hemispheres are equally competent at the onset of development and responses to faces become restricted to the right hemisphere as infants and children enlarge their visual world and learn new visual categories[8]. The organization of the final mosaic of specialized regions in the adult brain is determined through competition possibly weighted by inherent structural connectivity advantages[9]. For example, visual word-specific activation is left-lateralized in order to reduce the path length toward the oral language network, resulting in a competition between words and faces to occupy the same territory in the left hemisphere[10]. This idea is supported by evidence of more right lateralized responses to faces in normal readers compared to dyslexic children[11] and illiterate adults[12]. In both hypotheses, connectivity, maturation, and exposure have an influence on the brain's final organization; however, these hypotheses diverge on the initial organization of the brain. The former promotes initial neural specificities of genetic origin, which constrain the processing of the visual environment, whereas the latter emphasizes the role of the environment in determining the organization of the brain. This debate is not purely theoretical as plasticity might be reduced in areas committed to specific functions, explaining long-term effects of early sensory deprivation[13] and, more generally, inadequate early stimulation.

Faces are the first and most frequent visual stimulus to which infants are exposed, and face recognition is crucial to establish social bonding. Face perception is hypothesized to rely on both innate biases for orienting one's gaze to face-like stimuli and personal experience in discriminating faces of one's entourage[14-16]. From birth on, neonates discriminate their mother's face from a stranger's initially using predominantly the hairline and outer contour of the head[17,18]. They tolerate only a slight deviation from the frontal view in recognizing the same face[19]. During the first months after birth, they rapidly progress in recognizing novel faces, even when presented in different orientations[20], and perform better for ethnic faces with which they are most familiar[21] and the gender that is most represented around them[22-24].

What are the neural bases of this rapid and efficient learning? Is there already a right hemisphere advantage to process faces in infants? Electro-encephalography (EEG) is the easiest technique to study the infant brain. Two evoked-related responses (ERPs) components, the N290 and P400, have been reported to be modulated by face perception[25-28], and face discrimination[24,29-31]. Although a larger right response has been reported in some studies[26,32], these components are commonly measured bilaterally. Recently, 4-6 month-old infants were shown to recognize faces in different orientations in natural scenes, and the face-selective responses highlighted by a frequency-tagging approach appeared to be strongly right-lateralized[33], in agreement with hemispheric asymmetries described in adults using the same method[34].

Near-infra-red spectroscopy (NIRS) studies confirm an early right hemispheric superiority. Using a recording patch over the temporal areas in 5 to 8 month-old infants, Kakigi and collaborators

reported a bilateral response to canonical upright faces relative to a baseline of vegetable pictures[35-37], but a right hemispheric advantage emerged when canonical vs. scrambled faces[35] and upright vs. inverted faces[37] were contrasted. The response in the right hemisphere progressively enlarged along the third trimester of life, notably for other views of a face[38]. Positron emission tomography **(**PET) and functional magnetic resonance imaging (fMRI) studies in young children are surprisingly less conclusive. Responses to faces have been localized to the fusiform regions in infants [39,40] but might be less specific to such stimuli than later in life, as these regions were similarly activated by faces and objects in 3 to 8-month-old infants contrary to adults [40]. The reported fusiform activations were either not lateralized [40] or weakly right lateralized [39]. Note that in NIRS studies, measures from a large temporal recording patch were merged. This might increase the sensitivity to small but consistent differences in each voxel from the ventral temporal areas but also sum up activity from different regions involved in face perception – i.e., the fusiform gyrus, the occipital face area and the posterior superior temporal region – which were reported but not merged for analyses in the fMRI and PET studies. Face-specific activations measured with fMRI in the ventral visual areas remain weak over a long period. Hardly observed in young children at 5-8 years of age[41] (but see Cantlon et al., 2011[42]), face-selective responses in the fusiform gyrus progressively enlarge throughout childhood, with a stronger right-lateralization in adults than in children[43-45]. A longer period of cortical microstructural changes in the posterior fusiform gyrus than in neighboring areas might support this long functional development[46].

Another way to establish each hemisphere's specificities is to exploit visual hemifield presentation: due to the organization of the visual pathways, only the contra-lateral hemisphere is informed on the stimulus until inter-hemispheric transfer occurs. In adults, reaction times for recognizing faces are faster when presented in the left hemifield (right hemisphere) than in the right hemifield while opposite results are obtained for word reading[47]. A left hemifield alexia reported in a patient with a lesion of the splenium[48] and the requirement of a left hemifield presentation to encode face identity across different orientations[49] are some of the examples which establish the superiority of one or the other hemisphere in adults and the need to transfer information to the specialized hemisphere for correct processing.

In infants, a left hemifield (i.e. right hemisphere) superiority was observed in three-month-olds, who oriented faster to familiar faces presented in the left hemifield than in the right[52,53]. A robust left hemifield superiority was also reported when the two faces were differing in eye size and eye orientation but a reverse effect (right hemifield- left hemisphere advantage) was observed when differing for by their eye shape in 4 to 10 month-old infants[54]. However, behavioral experiments cannot disentangle the following hypotheses: (1) both hemispheres perform the task but the left hemisphere is slower than the right, or (2) only the right hemisphere performs the task, revealing a radical dissociation as reported in adults.

Furthermore, if both hemispheres have different competencies, what is the role of the corpus callosum in amplifying or reducing these differences? This large pathway is completed during gestation[55], but its myelination continues until adolescence. Concerning the splenium fibers which connect visual regions, their myelination begins after the third postnatal month and rapidly progresses until the end of the first year[56,57] and possibly later on[58] . We may thus wonder whether this rapid maturation has a role in the development of left-right functional asymmetries allowing the most competent hemisphere to inhibit the other[59] or whether the callosal fibers only follow the maturational calendar of the connected visual areas.

Exploring the question of inter-hemispheric transfer, de Schonen and collaborators used a conditional learning paradigm in which infants learned to orient to an upper toy for one image and to a lower toy for another image. The images were first presented in one hemifield, then the authors measured whether the number of trials to reach the learning criterion was reduced for the same images secondarily presented in the other hemifield. A transfer was observed at 6 months when a face and a scrambled face were presented[60] but no inter-hemispheric transfer was observed before 24 months of age when two faces were used[53,54,61]. Therefore, reconsidering the first study, Liegeois et al. (2000) hypothesized that face categorization was probably conveyed through subcortical pathways to both

hemispheres and that face identity encoding required the corpus callosum, which was not fully functional before the second year of life. By contrast, Sann and Streri (2007) showed that neonates were able to transfer tactile and haptic information from one hand to the other[62]. The discrepancy between these results might be related to a different experimental sensitivity but more probably to the fibers connecting perirolandic regions being consistently more mature than splenium fibers from gestation on[63].

We thus aimed to reconsider these questions thanks to the opportunities offered by coupling structural and functional brain imaging techniques**.** We used diffusion MRI and high-density (128 channels) EEG in a group of 40 infants aged between 1 to 6 months, 13 of them completing both diffusion MRI and EEG tests. We first assessed the influence of connectivity on the infant's visual responses by correlating the speed of visual ERPs with diffusion tensor imaging (DTI) measures of white matter maturation obtained in the same infants. DTI can be used to follow white matter myelination throughout infancy due to its sensitivity to water molecule diffusion[6,64-67]. Water diffusion becomes preferentially channeled along axons with the progressive myelination of the fibers, resulting in a decrease in transverse diffusivity. In parallel, myelination accelerates the conduction of neural responses, which can be captured on the scalp through decreases in the latencies of the ERP components. For central stimuli, for instance, the latency of the first visual evoked component (P1) shifts from around 300 ms at birth to about 120 ms after 12 weeks of age[68]. In a previous study, we related this acceleration to the myelination of the optic radiation and, notably, to a decrease in transverse diffusivity[6]. In the present study, we compared the P1 latency for central and lateralized stimuli, and correlated the speed of the P1 response appearing on the contralateral hemisphere to the transverse diffusivity of the optic radiation. We also measured the inter-hemispheric transfer time (IHTT) as the difference between the contra- and ipsi-lateral P1 and correlated its related speed with the transverse diffusivity in the splenium fibers that connect the visual areas. In adults, a shorter IHTT has been shown to correlate with lower mean diffusivity[69], higher fractional anisotropy[70], and higher axon diameter[71] in the posterior part of the corpus callosum.

Second, we evaluated each hemisphere's competency in discriminating lateralized faces. Are both hemispheres or is only the right hemisphere reacting to a new face? How is information on face identity exchanged between hemispheres? Infants were thus exposed to two streams of faces in the left and right hemifield. One face was assigned to one hemifield and was presented frequently (standard image). Occasionally deviant faces, defined as either a new face (new-deviant image) or the standard face of the other side (known-deviant image), were presented. The new-deviant condition was used to separately study each hemisphere's response to change and thus to compare their efficiency. Contrarily, the known-deviant condition was used to study the functional efficiency of the corpus callosum at this age. We hypothesized that if the corpus callosum is already efficient, the ispi-lateral face ("known-deviant" image) should be considered as familiar as the contra-lateral face (standard image), whereas if there is no inter-hemispheric transfer, it should be considered as novel as the "new-deviant" face.

Results:

An efficient inter-hemispheric transfer of early visual responses in infants

ERPs responses: Brain visual responses to faces were recorded with a high-density EEG system (128 channels) in infants aged between 5.6 to 23.6 weeks. 23 were tested with central faces (Figure 1). The P1 latency measured over mid-occipital areas decreased with age from 185 to 121 ms ($R^2 = 0.41$, $p < 0.001$ in 23 infants, Figure 2.a., c) and reached a plateau around 12 weeks of age (Figure 2. c). This decrease in P1 latency was better fitted with a 3rd degree polynomial ($R^2 = 0.72$, $p < 0.001$) than with a linear model (Akaike's information criterion [72]: AIC polynomial model = 179; AIC linear model = 189).

Lateralized faces were used in 40 infants (comprising the 23 infants mentioned above). An initial response over the contralateral hemisphere was identified followed by a response on the ipsi-lateral hemisphere (Figure 2. b.). The P1 latency for contralateral responses to lateralized faces was slower than the responses for central faces ($t(1,22) = 9.3$, $p = 0.004$) and linearly decreased with age

(from 341 to 137 ms, $R^2 = 0.51$, $p < 0.001$ in 40 infants; Figure2.c). The IHTT similarly decreased from 315 to 84 ms ($R^2 = 0.39$, $p < 0.001$, Figure 2. c). The age-related slopes did not differ between the contralateral P1 latency and IHTT ($t(1,39) = 1.5$, $p > 0.1$). Finally, P1 latencies and IHTT were similar for faces in the left and right hemifield (P1: $t(1,39) < 1$, $p > 0.1$; IHTT: $t(1,39) = -1.5$, $p > 0.1$).

DTI measures: The maturation of the optic radiations and commissural fibers was studied in 22 infants imaged with diffusion MRI and compared to the equivalent tracts in the auditory domain to control for general vs domain-specific maturation. We dissected the optic and acoustic radiations (OR, AR), the visual and auditory callosal fibers (vCC, aCC) with probabilistic tractography (Figure 3. a.). In all tracts, DTI transverse diffusivity significantly decreased with age (Figure 3. b, $-0.87<r<-0.68$, $p<0.001$). Using partial correlations to remove global effects of the infants' ages (Table 1), we observed significantly correlated maturational patterns for the microstructural properties of optic radiations and visual callosal fibers ($r(\text{OR-vCC} \mid \text{age}) = 0.78$, $p<0.001$) and for the visual and auditory callosal fibers ($r(\text{vCC-aCC} \mid \text{age}) = 0.74$, $p<0.001$). These results suggest that bundles belonging to the visual network mature in synchrony as do callosal fibers connecting visual and auditory regions in the splenium. Finally, transverse diffusivity was lower in the left relative to the right hemisphere in both optic radiations ($t(21) = -5.3$, $p<0.001$) and auditory radiations ($t(21) = -5.1$, $p=0.001$), suggesting an advanced maturation in the left hemisphere tracts.

In a subgroup of 13 infants studied with both the ERP lateralized paradigm and diffusion MRI, we investigated whether the conduction speed of visual evoked responses (i.e. distance/latency, see method) was related to the maturational properties of the underlying pathways. Using partial correlations to account for infants' ages (Table 1), we observed that the speed of the contralateral P1 was related to the maturation of optic radiations ($r(\text{speedP1} - \text{OR} \mid \text{age}) = -0.65$, $p = 0.021$, Figure 3.b), while the speed of inter-hemispheric transfer was related to the maturation of visual and auditory callosal fibers ($r(\text{speed}_{\text{IHTT}} - \text{vCC} \mid \text{age}) = -0.64$, $p = 0.025$, Figure 3. c.; $r(\text{speed}_{\text{IHTT}} - \text{aCC} \mid \text{age}) = -0.65$, $p = 0.021$).

Altogether, these results reveal that the inter-hemispheric transfer of early visual responses is already efficient during infancy and is strongly related to the maturation of the underlying callosal fibers.

An efficient discrimination of left-hemifield faces

In the second step of this study, we evaluated whether infants were able to discriminate faces that were presented either in the left or right hemifields (Figure 1.c). Figure 4 shows the grand average ERP on the ipsi and contra-lateral clusters for each stimulated visual hemifield, all conditions merged (standard, new-deviant and known-deviant faces). We focused our ERP analyses on the P1 to examine the effects of low-level features, and on the N290 and P400 components which are the classical components related to face perception in the infant literature[25] (Figures 4-6 and S1). In each of the 40 infants tested with the lateralized paradigm, we averaged the voltage over three 100 ms time windows (P1: [150-250] ms; N290: [300-400 ms]; P400: [450-550 ms]) and over symmetrical left and right clusters of 10-electrodes in the occipito-temporal regions (see method for the choice of temporal windows and electrodes). We entered these values into separate analyses of variance (ANOVA) with condition (3-levels), hemifield (2-levels) and cluster (2-levels) as within-subject factors. Considering the P1, the ANOVA revealed a significant interaction hemifield by cluster ($F(1,39)=26.5$, $p<.001$) because, as expected for a lateralized stimulation, the contralateral response was larger than the ipsilateral response (for each hemifield, $p<.001$). A modest trend for an interaction condition by cluster was also present ($F(1,39) = 2.6$, $p = 0.08$). Considering the N290, there was a main effect of condition ($F(2, 78) = 3.4$, $p = 0.039$), a marginally significant effect of cluster ($F(1,39) = 3.6$, $p = 0.065$), a significant interaction hemifield by cluster ($F(1, 39) = 15.1$, $p < 0.001$) and a marginally significant interaction between condition and cluster ($F(2, 78) = 2.7$, $p = 0.074$). Considering the P400, only a main effect of hemifield was observed ($F(1,39) = 5.1$, $p = 0.030$). We then analyzed each hemifield separately.

Responses to left hemifield faces. Considering the P1, there was no effect of condition on the contralateral ($F(2, 78) = 2.4$, $p > 0.1$) and ipsilateral hemisphere ($F(2, 78) < 1$). For the N290, an effect of condition was observed over the contralateral right cluster ($F(2, 78) = 5.1$, $p = 0.016$) but not over the ipsilateral left cluster ($F(2, 78) < 1$). Post-hoc t-test analyses for paired conditions indicated that the N290 amplitude was larger (i.e. more negative) for new-deviant faces than for standard and known-deviant faces (respectively: $t(1,39) = -2.2$, $p = 0.031$; $t(1,39) = -2.7$, $p = 0.014$) (Figure 5. a, Figure 6. a., Table 2), whereas no difference was detected between standard and known-deviant faces ($t(1,39) < 1$). Thus, infants discriminated faces presented in their left hemifield, whereas standard faces from the other side (right hemifield) did not elicit a novelty response, demonstrating that face information had been transferred between hemispheres. The N290 amplitude difference between new and standard faces became larger with age ($r = -0.38$, $p = 0.047$, Figure 6. c.) due to an increase of the N290 absolute amplitude in response to new-deviant faces. No age effect was observed for the difference between new- and known-deviant faces ($r = -0.16$, $p > 0.1$, Figure 6. c.).

The same pattern was seen for the P400. An effect of condition was observed over the contralateral right cluster ($F(2, 78) = 3.9$, $p = 0.047$) but not over the ipsilateral left cluster ($F(2, 78) < 1$). The P400 was significantly weaker for new faces relative to standard faces ($t(1,39) = -2.3$, $p = 0.042$) and known-deviant faces ($t(1,39) = -2.7$, $p = 0.029$), whereas responses for standard and known-deviant faces did not differ ($t(1,39) < 1$) (Figure 5. a., Figure 6. a.). The difference between new and standard faces tended to become larger with age despite not surviving multiple comparison corrections ($r = -0.26$, $p > 0.1$) (Figure 6. c.). No age effect was observed for the difference between new- and known-deviant faces ($r = 0.16$, $p > 0.1$, Figure 6. c.).

Responses to right hemifield faces. There was no significant effect of condition for the P1, N290 and P400 responses, either in the contralateral left or in the ipsilateral right clusters (Figure 5. b., 6. b., Table 2). As we were surprised by this result, we looked for putatively delayed effects. By visually inspecting the time-series, we selected two later time-windows (t1: [750-850 ms], t2: [1050-1150 ms]). Again no effect of condition was found (on the contralateral left cluster: t1: $F(2,79) = 1.6$, $p > 0.1$; t2: $F(2,79) = 1.7$; $p > 0.1$; on the ipsilateral right cluster: t1: $F(2,79) < 1$; t2: $F(2,79) < 1$), although new-deviant faces tended to evoke more positive responses than standard faces on the contralateral left cluster (t1: $t(1,39) = 1.8$, $p = 0.071$; t2: $t(1,39) = 1.9$, $p = 0.065$) but not the ipsilateral right cluster ($t(1,39) < 1$, for both t1 and t2). Responses for known-deviant faces did not differ from the two other conditions ($p > 0.1$ for t1 and t2 on both contra- and ipsi-lateral clusters). Thus, no reliable difference between conditions was detected in the contra-lateral and ipsi-lateral hemisphere revealing that infants were not able to discriminate faces presented in their right hemifield either in the left or right hemisphere.

Finally, we studied whether the responses to standard faces presented in the right and left hemifield were different. The amplitudes of the P1, N290 and P400 were similar for the left and right hemifield, on the ipsi- and contra-lateral clusters ($p > 0.1$) confirming not only that both hemispheres were processing the stimuli but also that responses to left standard faces were not reduced relatively to right standard faces.

Discussion:

By combining structural and functional measures using multi-modal imaging, we uncovered several aspects of visual development in human infants. We first confirmed the interdependency between DTI measures of white matter maturation and the speed of the neural responses, not only at the level of projection tracts, such as the optical radiations, but also at the level of cortico-cortical tracts, such as the corpus callosum. In particular, the myelination of the splenium fibers supports the progressive acceleration of information transfer between hemispheres during the first post-natal semester. Second, we revealed that the right hemisphere, but not the left, discriminates faces presented in the contralateral hemifield. The response to a new face enlarged and accelerated with age only in the right hemisphere revealing an improvement in the right hemisphere's processing ability whereas the left hemisphere remained unresponsive to face differences. Third, new faces presented in the right hemifield did not evoke any discriminative response neither in the left nor in the

"competent" right hemisphere highlighting the still poorly functional inter-hemispheric transfer at this age. Finally, we observed no evidence for an inhibitory role of the corpus callosum on the left responses as the P1 latencies, the IHTT and the N290/P400 amplitudes for standard faces did not differ for left and right hemifield presentations in either hemisphere.

First, we asked whether fiber-specific microstructural maturation correlates with the acceleration of evoked responses. Age-dependent acceleration of the P1 response has been repeatedly reported for central visual stimuli[6,68,73], reflecting the increasing efficiency of the visual pathway from the retina and LGN to the visual cortices. Here, lateralized stimuli evoked delayed P1 responses relative to central stimuli probably because of the micro-architectural differences between the fovea composed of very dense cones and the peripheral retina primarily containing rods[74,75]. P1 acceleration persisted after 12 weeks of age for lateralized stimuli whereas the adult latency was already reached for central stimuli at this age. The speed of the early visual responses for lateralized stimuli was related to the transverse diffusivity in the optic radiation independent of age, as we had previously demonstrated for central stimuli[6]. Thus, myelination of the optic fibers is one of the major factors improving visual efficiency during the first semester of postnatal life beyond the maturation of the peripheral paths and of V1.

The correlation between the structural and functional measures of development was also seen for callosal connections and the speed of inter-hemispheric transfer. We measured IHTT for the first time in infants and related its speed increase to the maturation of splenium callosal fibers connecting occipital regions. IHTT shortened from 300ms in the youngest to 84ms in our oldest infants. This delay is notwithstanding far longer than in adults: 7-13 ms in response to checkerboards[76], 15 ms in response to white squares[70], 30 ms in in response to faces[77], but is in the expected range for thin unmyelinated callosal fibers whose conduction delays are between 100 and 300 ms[78]. The maturation of visual callosal fibers was significantly correlated with the maturation in the optic but not the auditory radiations uncovering domain-related rather than a general maturation. Thus, diffusion MRI might be a practical tool for following the efficiency of white matter pathways during development and to reveal neural connectivity through correlated maturation in normal but also pathological populations.

Next, we focused on our main goal and studied each hemisphere's ability to process faces by using two streams of faces in the left and right visual hemifields. We are confident that almost all faces were seen in a lateralized hemifield based on several arguments. First, *at the experiment level*, the short duration of face presentations (250ms) was below the time delay for a saccadic eye movement at this age which is about 400ms in 4 month-old infants[79]. The randomized delay between faces prevented infants from predicting the exact stimulus onset and orienting their gaze to the corresponding hemifield. We further inspected the video recordings of the infants' behavior during the experiment to verify that they were continuously centered with respect to the screen and that they did not shift their gaze toward a side of the screen. Second, the identification of *contralateral P1 responses* to left and right faces confirmed that infants were focused on the central distractor at the onset of the lateralized stimulation (see figure 2 and 4). This response was followed by *ipsilateral responses*, and the significant correlation between the IHTT and the maturation of the splenium callosal fibers validates that we were measuring a genuine transfer of information between hemispheres. Finally, the similar succession of components (P1, N290 and P400, figure 4) observed over each hemisphere contralateral to the stimulation confirms that each hemisphere was perceiving and processing the contralateral face. Altogether these arguments support the reliability of our experimental paradigm to test each hemisphere separately in infants.

With this paradigm using lateralized stimuli, we were able to uncover striking differences between left and right hemisphere capabilities. We recorded discrimination responses only in the right hemisphere for new faces presented in the contralateral left hemifield, revealing *a contrario*, a surprisingly incompetent left hemisphere. If any evidence of face discrimination capacity for the left hemisphere existed in this task, it was a delayed, weak and hardly significant response around [750-850] and [1050-1150] ms post-stimulus, which contrasts with the earlier and robust N290 and P400 responses in the right hemisphere. It might be possible that the discrimination between our face

images was done on low-level cues. However, if such were the case, we should have expected an early difference at the level of the P1 as shown by Rossion and Caharel in adults[80]. This was indeed not the case (i.e. no effect of condition at the level of the P1), but further studies might verify this point by using scrambled images as controls as in De Heering and Rossion[33].

In adults, the left visual hemifield superiority for faces is related to right-left fusiform face area (FFA) asymmetrical activation for face recognition[81]. In infants, this hemispheric difference was first asserted by de Schonen and her collaborators based on behavioral studies in which they measured the latency of gaze orientation toward faces presented in the left and right visual hemifield[52,53]: four-month-old infants oriented faster to their mother's face than to a stranger's presented in the left hemifield. Furthermore, the same infants oriented faster toward their mother's face presented in the left rather than their mother's face presented in the right hemifield. In a second task, the infants had to associate the position of a rewarding toy (above or under the screen) with the identity of a face (mother or stranger) presented within the right or left hemifield. They succeeded only when the faces were presented in the left hemifield and thus processed by the contralateral right hemisphere (i.e. 72% vs 17% of infants reached the learning criterion for left vs right hemifield faces; percentages computed from table 4 in de Schonen and Mathivet). Our results confirm that infant's orienting failures for right-hemifield faces in this study were related to a genuine difficulty in discriminating the two faces in that hemifield rather than to subsequent difficulties in associating each face with the spatial position of the reward.

In NIRS studies, a right hemispheric superiority was robustly observed when configural perception was tested in 5 to 8-month-olds (i.e. upright vs inverted faces[37] and canonical vs scrambled faces[35]) with a progressive development of a response for other views of the face during the second semester of infancy[38]. Similarly, de Heering and Rossion[33] who used a rapid presentation of faces in different sizes and view-points relative to various visual categories reported a strong right hemisphere advantage in 4-6 months. These results suggest that face categorization mainly relies on the right hemisphere from the first months of life on. However, discrimination between different faces measured with NIRS induced bilateral responses in 7 to 8-month-olds[36,82,83]. Here, our paradigm with rapid presentation of faces and divided attention between the two hemifields may have amplified the differences in face processing abilities of the left and right hemisphere much in the same way dichotic presentation reveals the superiority of the left hemisphere for speech. The left hemisphere has been shown to be sensitive to face features[54], which may require a foveal analysis and a longer time to be discriminated, whereas the fast presentation outside the fovea in our paradigm might have favored a rapid configural analysis done by the right hemisphere[54]. The left and right hemifield faces were never directly in competition but were successively presented with a random delay of 550 to 950 ms. In adults, this delay would be sufficient to reallocate attention from one side to the other but probably not in infants because of their difficulties in rapidly disengaging and reengaging their attention. It may have amplified the spontaneous advantage of the left hemifield.

The N290 amplitude increased with age in response to new faces compared to standard faces, whereas the P400 amplitude showed the opposite effect. This pattern suggests an acceleration of the discrimination response shifting from the P400 to the N290 time-range, and supports the hypothesis that both components are precursors of the adult face-specific N170 component[28]. This acceleration is probably related to the more refined representations of faces in the infant's environment and of their distinctiveness[21-24,84]. It is noteworthy that the P1 for central stimuli reaches the adult values around 12 weeks of age (figure 2c), at the same time infants start to become sensitive to second-order relations[85,86]. This better sensory encoding certainly might help infants perceive more subtle differences.

Le Grand et al. (2003) reported that visual input to the right hemisphere during the first post-natal months was necessary for adults to perceive second-order relations: adults with an early left cataract were unable to perceive a change in the spacing between both eyes as well as between the eyes and the mouth in successive pictures of faces contrary to adults with an early right cataract. However, they were able to perceive changes in the contours of the face or internal face features (eyes and mouth) similarly to normal participants[13]. Combined with our results in which only the right

hemisphere benefited from a discrimination improvement during the first semester of life, these findings might point to a genuine left-hemispheric difficulty in processing these relations in a face space and thus to a different microstructural organization of the left and right fusiform regions, probably of genetic origins with a critical window of learning for the right FFA. Within the fusiform gyrus, Weiner et al[87] have described four regions cyto-architectonically dissociable, and associated with specific functional domains: FG2 and FG4 comprising face and word specific areas[87]. As the MRI signal is sensitive to water, but also to iron and myelin, quantitative MRI can provide markers of maturation of the gray matter[5]. The maturational calendar of these regions and of the neighboring areas might reveal the microstructural differences that may underlie this functional asymmetry.

Finally, we investigated the efficiency of the inter-hemispheric transfer of visual information. Right-lateralized faces were not discriminated by the left hemisphere. Does this result imply that infants do not process faces presented in their right visual hemifield at all? If such were the case, the right hemifield standard face should have been processed as a new face by the right hemisphere when occasionally presented in the left hemifield (known-deviant condition); however this effect was not present in our study. On the contrary, we observed no difference between the left and right hemifield standard faces regardless of presentation side or cluster, revealing that the transfer of information of face features was successful when a face was repeated. One could oppose this interpretation by suggesting that the infant may have shifted their gaze to the right hemifield and seen the standard face on this side; however such occurrences, if any, were rare given our visual controls and likely just as rare as the new-face condition. Thus, without inter-hemispheric transfer, the known-face should have elicited a similar response to that of a new face. However, if the inter-hemispheric transfer had been fully efficient, the new face perceived by the left hemisphere should have been transferred to the competent right hemisphere to be discriminated. Yet, we found no significant difference between conditions over the ipsilateral cluster, even at a later time-window for faces presented in the right hemifield. The long IHTT in our group, relative to adults, may have hindered a correct processing of a rare image, whereas the repeated image may have progressively succeeded in obtaining a robust representation in the right hemisphere. Inter-hemispheric transfer is thus imperfect at this time period and may remain so until the end of the second year of life, hereby explaining the behavioral results. Indeed, the cognitive tasks used in two previous behavioral studies investigating trans-callosal transfer were complex: one was based on similarity judgment between two visual items presented simultaneously in the two hemifields[61], and the second on the number of trials needed to learn to discriminate two visual items once the other hemisphere has already learned to discriminate them [53].

Conclusion:

Exploiting multimodal imaging in infants, we have demonstrated that lateralized brain processes are not a property of the adult human brain but are observed from the first post-natal weeks on, likely due to structural specificities in the genetically specified left-right hemisphere architecture. We have also highlighted that an efficient transfer of visual information between hemispheres emerges before 6 months of infancy, but this transfer is still not fully efficient at this age and likely continues to improve over the course of several months, considering the extended maturation of the corpus callosum. Because our goal was to assess the functional improvements in relation with structural development, our age range extends over the first post-natal semester and we exploited the wide variation in the P1 latency. The N290 and P400 latencies are probably also accelerating, introducing inter-subject variability and possibly impinging upon statistical comparisons. Further studies should examine responses to right hemifield faces in a more homogeneous group but also at a later age in order to understand how the left hemisphere, and its abilities in featural analyses[54], becomes integrated in the face network. Identifying the anatomo-functional substrates of early visual development is crucial to understanding possible deviations from this normal trajectory and long-term effects of early damage to the visual system.

Materials and Methods:

We report results obtained in two groups. A first group of infants was studied with both EEG and diffusion MRI to study the functional maturation of visual responses for lateralized stimuli in

relation to the structural maturation of white matter pathways. A second group of infants was tested only with EEG to complete our initial analyses on face discrimination using lateralized stimuli and also to study responses for central faces.

Subjects

The first group consisted of 24 healthy full-term infants aged between 5.8 to 22.4 weeks (mean 14 ± 5.9 weeks, 11 girls). They were first scanned with MRI and then underwent EEG recordings within a week. Two infants had artifacted MRI images, 3 were not tested with EEG because their parents were unable to return in the predetermined delay, and 4 were rejected due to excessive movement during EEG. Thus, 22 infants were included in the structural analyses (mean age: 13.8 ± 4.2 weeks), 15 infants in the ERPs analyses (mean age: 15 ± 4.1 weeks), and 13 infants provided good MRI and EEG data to analyze the correlations between DTI parameters and ERPs latencies (mean age: 14 ± 4.3 weeks).

The second group of 25 healthy full-term infants (from 5.6 to 23.6 weeks old, mean age: 13.9 ± 5 weeks, 14 girls) was only tested with EEG. Twelve additional infants were excluded due to insufficient data quality. These 25 infants were merged with the 15 infants described above for a total of 40 infants in whom we studied electrophysiological responses to lateralized face presentations. Out of the 25 infants of the second group, 23 of them were presented with additional centered faces during the experiment.

The study was approved by the ethical committee for biomedical research. All of the infants' parents were informed about the content of the experiment as well as its goals and gave written informed consent before starting the experiment.

MRI acquisition and post-processing of diffusion images

Acquisitions were performed during spontaneous sleep in a 3T MRI system (Tim Trio, Siemens Healthcare, Erlangen, Germany), equipped with a whole-body gradient (40mT/m, 200T/m/s) and a 32-channel head coil. T2-weighted (T2w) images were acquired in infants using a 2D turbo spin echo sequence (spatial resolution = 1x1x1.1mm^3) [88]. A diffusion-weighted spin-echo EPI sequence was used with 30 orientations of the diffusion gradients applied with b=700s.mm^{-2}. Fifty interleaved axial slices covering the whole brain were acquired with a 1.8mm isotropic spatial resolution, leading to a total acquisition time of 5min40s which is reasonably short for unsedated infants[7].

After correction for motion artifacts with Connectomist software[89,90], probabilistic tractography was performed based on a 2-crossing-fiber diffusion model over individual brain masks with FSL software[91]. Using individual seed regions, several tracts were dissected: left and right optic radiations and visual callosal fibers from the visual network as well as acoustic radiations and auditory callosal fibers from the auditory network for comparative purposes. Seeds were localized at the level of lateral geniculate nucleus (LGN) and occipital regions for optic radiations, and at the level of medial geniculate nucleus (MGN) and auditory regions for accoustic radiations. Seeds for callosal fibers were located in left and right primary visual/auditory areas and fibers connecting these primary areas should pass through the corpus callosum splenium. Following the estimation of the diffusion tensor, DTI maps (fractional anisotropy FA, mean <D>, transverse $\lambda_\perp$ and longitudinal $\lambda_{||}$ diffusivities) were computed for each subject. Averaged parameter X was calculated for each tract by taking into account fiber density on the tract probability map[92]:

$$\bar{X} = \frac{\sum^i Pr_i \times X_i}{\sum^i Pr_i},$$

where i denotes the tract voxels, Pr_i is the fiber density at voxel i, and X_i is the value of the DTI parameter at voxel i. In white matter, DTI parameters are affected by axonal organization, compactness and myelination. We focused on transverse diffusivity which has been shown to be the best DTI marker of myelination [6,66,67].

EEG protocol

Experimental paradigm

Colored front faces of four female and four male adults with neutral expressions were used as visual stimuli. Six of these images were used for lateralized presentation and two for centered presentation. The image presentation was driven by E-Prime (Psycho-logical Software Products, Harrisburg, PA). The infants' eyes were attracted to the center of the screen by a rotating colored bull's-eye which remained at the center of the screen during the whole experiment (Figure 1).

Lateralized paradigm: Two streams of face images were presented at the left and right side of the rotating bull's-eye (Figure 1b-c). The center of the image was at ~7.5 degrees of eccentricity from the infants' center of view, its inner/outer edges at ~3.1/12.5 degrees of eccentricity for an infant sitting at about 60 cm from the screen. Each image was presented for 250 ms. The left and right images were presented asynchronously in an alternating fashion with a variable delay between images (550 to 950 ms post-offset of the image with a 50 ms step) to avoid anticipatory looks to the sides. Each stream included three types of images: a side-assigned face image (standard), a novel face (new-deviant), or the face commonly assigned to the other side (known-deviant). Inside a block, the faces were either all female or all male. Two similar paradigms but with different trial organizations were used for the two groups of infants.

First group (15 infants): To familiarize infants with the experimental paradigm and for them to learn the face-side assignment, 8 standard trials with side-assigned faces were first presented on each side (habituation phase). Then in a test phase, 54 trials were presented on each side, with a succession of 18 3-trial structures: 2 standard trials and the third trial being randomized chosen among either a standard, new- or known-deviant condition (Figure1. e.). Over the 54 trials, 42 (77.8 %) were thus standard trials, and 6 (11.1%) were new- or known-deviant trials. Each block included 124 trials (2 sides x (8 habituation + 54 test) trials), out of which 80.6 % were standard, 9.7 % new-deviant and 9.7 % known deviant. The whole experiment comprised 4 blocks alternating between female and male faces (9 mins).

Second group (25 infants): In the first group, the side of the first block image was not counterbalanced across infants, implying that the critical third image of the 3-trial structure (standard vs new- vs known-deviant faces) was always presented on the left side before the right side. In the second group, we controlled for trial order, such that: 1. Deviant trials were preceded by a similar number of standard trials on both left and right sides. 2. No two successive deviant faces at the same or opposite sides were allowed. Infants were presented with 4 blocks of 80 trials at each side (60 standard, 10 new-deviant, 10 known-deviant). As for the first group, 8 standard trials were presented at the beginning of each block in each hemifield, leading to 176 trials per block (2 sides x (8 habituation + 80 test) trials), out of which 77.3 % were standard, 11.4 % new-deviant and 11.4 % known-deviant.

Central paradigm (23 infants) a): We took advantage of this second group to test infants' responses to centered stimuli. 4 additional blocks of 30 trials (2 images with female and 2 with male faces) were presented after the blocks with lateralized stimuli. One female and one male face, not used during the lateralized paradigm, were presented at the center of the screen for 250 ms, spaced by a random interval of 250-550 ms during which the colored bull's-eye was presented (Figure1. a). The total duration of the second experiment (lateralized + centered paradigms) was at most 15 min.

EEG data acquisition

An EEG recording net comprising 128 electrodes (EGI, Eugene, USA) with a reference on the vertex was placed on the infants' heads relative to anatomical markers. Infants were seated on their parents' laps in front of the screen in a shielded EEG room. Music was continuously played behind the screen to attract the infants' attention toward the screen. If an infant was distracted, the experiment was briefly interrupted and the experimenter focused her/his attention back toward the screen. If it was not possible, the experiment was prematurely terminated. A camera placed above the screen recorded the infants' position and looking direction throughout the experiment. EEG was

continuously digitized at a sampling rate of 250 Hz during the whole experiment (net amp 200 system EGI, Eugene, USA).

EEG processing and ERP analyses

EEG pre-processing

EEG recordings were band-pass filtered between 0.5 and 20 Hz on the EGI recording station, then exported to be processed using MATLAB toolboxes: EEGLAB[93] and Brainstorm[94]. The signal was segmented into epochs of 1700 ms, [-200, +1500] ms relative to the onset of each face presentation. Channels contaminated by movement or eye artifacts were automatically rejected on a trial by trial basis based on amplitude variations inside an epoch: each channel epoch was rejected when the fast average amplitude exceeded 250 µv, or when deviation between fast and slow running averages exceeded 150 µv. Electrodes were rejected if they were marked as bad in more than 70% of the epochs, and trials were rejected if more than 50% of the electrodes were marked bad. Recordings were then re-referenced by subtracting the average activity of all channels over the brain to obtain average-reference recordings, then baseline-corrected by the 200ms preceding the onset of the image presentation. On average, we obtained 171/170 correct trials respectively for the left/right hemifield faces in the first group of infants, and 72/71/37 for the left/right/center location in the second group. For each infant, trials were first averaged by stimulus side (i.e., left/right/center) in order to evaluate the early visual ERP responses (i.e. P1). Then trials were averaged by condition (standard faces, new- or known-deviant faces in the left and right hemifield) to study face discrimination.

Early visual perception

P1 latencies: For left/right hemifield presentation, we evaluated the latency of the contralateral and ipsilateral P1 across the two groups (15+25=40 infants). On the grand average topography, we identified two symmetrical clusters of five electrodes around O1 and O2 where early visual responses were observed independent of infants' ages. We averaged the time-series across the electrode clusters in each infant and measured the latencies of the following components (Figure 2. b): P1 as the first positive peak in the hemisphere contralateral to the image, and P1 ipsi as the first positive peak appearing after P1 in the hemisphere ipsilateral to the stimulation. The inter-hemispheric transfer time (IHTT) was defined as the latency difference between these two peaks ($IHTT = Latency_{P1\ Ipsi} - Latency_{P1}$). For central faces, P1 latency was identified in each infant as the first positive peak over a cluster of 6 mid-occipital electrodes surrounding Oz (Figure 2. a).

Effect of age on P1 latencies and transverse diffusivity: We first assessed the effect of age on functional and structural measures: i.e. contralateral *P1*, *IHTT* and central *P1* on one hand, and on transverse diffusivity in optic/auditory radiations and visual/auditory callosal fibers on the other hand. To evaluate domain-specific maturational patterns beyond a general effect of age, we computed partial correlations (controlling for age) between transverse diffusivity measures for the 4 pairs of tracts. We used a false discovery rate (FDR) approach to correct for the number of comparisons. Finally, we tested hemispheric asymmetries in the optic and acoustic radiations with paired t-tests on the transverse diffusivity in the left and right tracts.

Relationships between P1 latencies and tract-specific transverse diffusivity: We proceeded by examining the relationship between functional and structural measures of maturation. Because ERP latencies depend on the distance the neural signal has to travel in addition to the myelination of pathways, we computed conduction speeds of ERP responses (distance/latency) using anatomical distances in the brain. For contralateral P1 latency, we approximated the length of the optic radiations as the distance between the eyes and the occipital poles measured on each individual infant's T2w images as in our previous study[6] and computed the conduction speed of P1 ($Speed_{P1}$). For inter-hemispheric transfer time, we measured the length of the callosal fibers obtained by tractography and computed the speed of inter-hemispheric transfer ($Speed_{IHTT}$). To confirm the specificity of these results to the visual domain, we performed the same analysis but considering the acoustic radiations and auditory callosal fibers as surrogate tracts for $Speed_{P1}$and $Speed_{IHTT}$, respectively. We used FDR approach to correct for the four comparisons.

Discrimination of lateralized presented faces

To study face discrimination responses, we considered only the standard and deviant trials which were at the same position in the block structure. For the first group for which faces were presented in a 3-trial structure, we considered the third face of the structure which was either a standard, known-deviant or new-deviant face. In the second group to mimic the constraints imposed on deviant trials in the first paradigm, we selected the standard faces following at least 2 standard faces on the same or opposite side. The numbers of trials considered in each condition was therefore balanced. On average, we obtained 11/10/14 trials per subject for the new-deviant/ known-deviant/ standard conditions at each side. Epochs were averaged for each condition and side of presentation in each infant. As results were similar in the two groups, the data were merged.

In the literature, two face specific components, the N290 and the P400 recorded over the lower temporal regions, have been reported in infants [25]. We thus selected two clusters of 10 electrodes in the left and right inferior temporal regions extending from O1 to T5 electrodes on the 10-20 international system (as in[95]). For each experimental condition, we averaged the voltage over these electrodes and over a 100 ms time-window centered on each component's peak in each infant. The peaks were determined on the grand-average from merging all conditions and infants. Therefore, we analyzed the three visual components (P1, N290 and P400) on the following time-windows [150-250] ms for the P1, [300-400] ms for N290 and [450-550] ms for P400 (Figure 4). The time-windows are slightly delayed compared to the classical timing of N290 and P400 components as latencies are delayed for lateralized stimuli relative to central stimuli and also because our infant cohort is younger than those most commonly tested.

The voltage amplitudes were entered in three independent analyses of variance, each comprising three within-subject factors: condition (standard, known-deviant and new-deviant), electrodes (left and right cluster), and side of stimulation (left and right hemifield). We examined two effects of interest in post-hoc analyses using paired t-tests: 1. Whether the new-deviant condition was significantly different from the standard condition in order to demonstrate face discrimination capabilities. 2. Whether the known-deviant condition was significantly different from the new-deviant condition or from the standard condition in order to evaluate the efficiency of the inter-hemispheric transfer. Finally, we evaluated whether the face discrimination response was correlated with age using robust regression. We report significant effects with a p value below 0.05, once corrected for multiple comparisons using FDR correction.

Data Availability Statement:

The data and the analysis code that support the findings of this study are available from the corresponding author upon request.

References

1 Dehaene, S. *Reading in the brain: The new science of how we read*. (Penguin, 2009).

2 Rakic, P. Specification of cerebral cortical areas. *Science* **241**, 170-176 (1988).

3 de Schonen, S. & Mathivet, E. First come, first served: A scenario about the development of hemispheric specialization in face recognition during infancy. *Cahiers de Psychologie Cognitive/Current Psychology of Cognition* (1989).

4 Dehaene-Lambertz, G. & Spelke, E. S. The Infancy of the Human Brain. *Neuron* **88**, 93-109, doi:10.1016/j.neuron.2015.09.026 (2015).

5 Leroy, F. *et al.* Early maturation of the linguistic dorsal pathway in human infants. *J Neurosci* **31**, 1500-1506, doi:10.1523/JNEUROSCI.4141-10.2011 (2011).

6 Dubois, J. *et al.* Microstructural correlates of infant functional development: example of the visual pathways. *J Neurosci* **28**, 1943-1948, doi:10.1523/JNEUROSCI.5145-07.2008 (2008).

7 Dubois, J. *et al.* Exploring the Early Organization and Maturation of Linguistic Pathways in the Human Infant Brain. *Cereb Cortex* **26**, 2283-2298, doi:10.1093/cercor/bhv082 (2016).

8 Johnson, M. H. Functional brain development in humans. *Nat Rev Neurosci* **2**, 475-483, doi:10.1038/35081509 (2001).

9 Saygin, Z. M. *et al.* Connectivity precedes function in the development of the visual word form area. *Nat Neurosci* **19**, 1250-1255, doi:10.1038/nn.4354 (2016).

10 Dundas, E. M., Plaut, D. C. & Behrmann, M. The joint development of hemispheric lateralization for words and faces. *J Exp Psychol Gen* **142**, 348-358, doi:10.1037/a0029503 (2013).

11 Monzalvo, K., Fluss, J., Billard, C., Dehaene, S. & Dehaene-Lambertz, G. Cortical networks for vision and language in dyslexic and normal children of variable socio-economic status. *Neuroimage* **61**, 258-274, doi:10.1016/j.neuroimage.2012.02.035 (2012).

12 Dehaene, S. *et al.* How learning to read changes the cortical networks for vision and language. *Science* **330**, 1359-1364, doi:10.1126/science.1194140 (2010).

13 Le Grand, R., Mondloch, C. J., Maurer, D. & Brent, H. P. Expert face processing requires visual input to the right hemisphere during infancy. *Nat Neurosci* **6**, 1108-1112, doi:10.1038/nn1121 (2003).

14 Acerra, F., Burnod, Y. & Schonen, S. d. Modelling aspects of face processing in early infancy Developmental Science Volume 5, Issue 1. *Developmental Science* **5**, 98-117 (2002).

15 Gauthier, I. & Nelson, C. A. The development of face expertise. *Curr Opin Neurobiol* **11**, 219-224 (2001).

16 Morton, J. & Johnson, M. H. CONSPEC and CONLERN: a two-process theory of infant face recognition. *Psychol Rev* **98**, 164-181 (1991).

17 Bushnell, I. W. R., Sai, F. & Mullin, J. T. Neonatal recognition of the mother's face British Journal of Developmental Psychology Volume 7, Issue 1. *British Journal of Developmental Psychology* **7**, 3-15 (1989).

18 Pascalis, O., de Schonen, S., Morton, J., Deruelle, C. & Fabre-Grenet, M. Mother's face recognition by neonates: A replication and an extension. *Infant Behavior and Development* **18**, 79-85 (1995).

19 Turati, C., Bulf, H. & Simion, F. Newborns' face recognition over changes in viewpoint. *Cognition* **106**, 1300-1321, doi:10.1016/j.cognition.2007.06.005 (2008).

20 Cohen, L. B. & Strauss, M. S. Concept acquisition in the human infant. *Child Dev* **50**, 419-424 (1979).

21 Kelly, D. J. *et al.* Three-month-olds, but not newborns, prefer own-race faces Developmental Science Volume 8, Issue 6. *Developmental Science* **8**, F31-F36 (2005).

22 Quinn, P. C. *et al.* Infant preference for female faces occurs for same- but not other-race faces Journal of Neuropsychology Volume 2, Issue 1. *Journal of Neuropsychology* **2**, 15-26 (2008).

23 Quinn, P. C., Yahr, J., Kuhn, A., Slater, A. M. & Pascalils, O. Representation of the gender of human faces by infants: a preference for female. *Perception* **31**, 1109-1121, doi:10.1068/p3331 (2002).

24 Righi, G., Westerlund, A., Congdon, E. L., Troller-Renfree, S. & Nelson, C. A. Infants' experience-dependent processing of male and female faces: insights from eye tracking and

event-related potentials. *Dev Cogn Neurosci* **8**, 144-152, doi:10.1016/j.dcn.2013.09.005 (2014).
25 de Haan, M., Pascalis, O. & Johnson, M. H. Specialization of neural mechanisms underlying face recognition in human infants. *J Cogn Neurosci* **14**, 199-209, doi:10.1162/089892902317236849 (2002).
26 Gliga, T. & Dehaene-Lambertz, G. Structural encoding of body and face in human infants and adults. *J Cogn Neurosci* **17**, 1328-1340, doi:10.1162/0898929055002481 (2005).
27 Gliga, T. & Dehaene-Lambertz, G. Development of a view-invariant representation of the human head. *Cognition* **102**, 261-288, doi:10.1016/j.cognition.2006.01.004 (2007).
28 Halit, H., de Haan, M. & Johnson, M. H. Cortical specialisation for face processing: face-sensitive event-related potential components in 3- and 12-month-old infants. *Neuroimage* **19**, 1180-1193 (2003).
29 Key, A. P. & Stone, W. L. Processing of novel and familiar faces in infants at average and high risk for autism. *Developmental cognitive neuroscience* **2**, 244-255 (2012).
30 Peykarjou, S., Pauen, S. & Hoehl, S. 9-Month-Old Infants Recognize Individual Unfamiliar Faces in a Rapid Repetition ERP Paradigm Infancy Volume 21, Issue 3. *Infancy* **21**, 288-311 (2016).
31 Scott, L. S. Featural and configural face processing in adults and infants: a behavioral and electrophysiological investigation. *Perception* **35**, 1107-1128, doi:10.1068/p5493 (2006).
32 Scott, L. S., Shannon, R. W. & Nelson, C. A. Neural Correlates of Human and Monkey Face Processing in 9-Month-Old Infants Infancy Volume 10, Issue 2. *Infancy* **10**, 171-186 (2006).
33 de Heering, A. & Rossion, B. Rapid categorization of natural face images in the infant right hemisphere. *Elife* **4**, e06564, doi:10.7554/eLife.06564 (2015).
34 Rossion, B., Torfs, K., Jacques, C. & Liu-Shuang, J. Fast periodic presentation of natural images reveals a robust face-selective electrophysiological response in the human brain. *J Vis* **15**, 15 11 18, doi:10.1167/15.1.18 (2015).
35 Honda, Y. *et al.* How do infants perceive scrambled face?: A near-infrared spectroscopic study. *Brain Res* **1308**, 137-146, doi:10.1016/j.brainres.2009.10.046 (2010).
36 Nakato, E. *et al.* I know this face: neural activity during mother's face perception in 7- to 8-month-old infants as investigated by near-infrared spectroscopy. *Early Hum Dev* **87**, 1-7, doi:10.1016/j.earlhumdev.2010.08.030 (2011).
37 Otsuka, Y. *et al.* Neural activation to upright and inverted faces in infants measured by near infrared spectroscopy. *Neuroimage* **34**, 399-406, doi:10.1016/j.neuroimage.2006.08.013 (2007).
38 Nakato, E. *et al.* When do infants differentiate profile face from frontal face? A near-infrared spectroscopic study Human Brain Mapping Volume 30, Issue 2. *Human Brain Mapping* **30**, 462-472 (2009).
39 Tzourio-Mazoyer, N. *et al.* Neural correlates of woman face processing by 2-month-old infants. *Neuroimage* **15**, 454-461, doi:10.1006/nimg.2001.0979 (2002).
40 Deen, B. *et al.* Organization of high-level visual cortex in human infants. *Nat Commun* **8**, 13995, doi:10.1038/ncomms13995 (2017).
41 Scherf, K. S., Behrmann, M., Humphreys, K. & Luna, B. Visual category-selectivity for faces, places and objects emerges along different developmental trajectories. *Dev Sci* **10**, F15-30, doi:10.1111/j.1467-7687.2007.00595.x (2007).
42 Cantlon, J. F., Pinel, P., Dehaene, S. & Pelphrey, K. A. Cortical representations of symbols, objects, and faces are pruned back during early childhood. *Cereb Cortex* **21**, 191-199, doi:10.1093/cercor/bhq078 (2011).
43 Gathers, A. D., Bhatt, R., Corbly, C. R., Farley, A. B. & Joseph, J. E. Developmental shifts in cortical loci for face and object recognition. *Neuroreport* **15**, 1549-1553 (2004).
44 Golarai, G. *et al.* Differential development of high-level visual cortex correlates with category-specific recognition memory. *Nat Neurosci* **10**, 512-522, doi:10.1038/nn1865 (2007).
45 Peelen, M. V., Glaser, B., Vuilleumier, P. & Eliez, S. Differential development of selectivity for faces and bodies in the fusiform gyrus Developmental Science Volume 12, Issue 6. *Developmental Science* **12**, F16-F25 (2009).

46 Gomez, J. *et al.* Microstructural proliferation in human cortex is coupled with the development of face processing. *Science* **355**, 68-71, doi:10.1126/science.aag0311 (2017).
47 Rizzolatti, G., Umilta, C. & Berlucchi, G. Opposite superiorities of the right and left cerebral hemispheres in discriminative reaction time to physiognomical and alphabetical material. *Brain* **94**, 431-442 (1971).
48 Cohen, L. *et al.* The visual word form area: spatial and temporal characterization of an initial stage of reading in normal subjects and posterior split-brain patients. *Brain* **123 (Pt 2)**, 291-307 (2000).
49 Verosky, S. C. & Turk-Browne, N. B. Representations of facial identity in the left hemisphere require right hemisphere processing. *J Cogn Neurosci* **24**, 1006-1017, doi:10.1162/jocn_a_00196 (2012).
50 De Renzi, E. Prosopagnosia in two patients with CT scan evidence of damage confined to the right hemisphere. *Neuropsychologia* **24**, 385-389 (1986).
51 Landis, T., Cummings, J. L., Christen, L., Bogen, J. E. & Imhof, H.-G. Are unilateral right posterior cerebral lesions sufficient to cause prosopagnosia? Clinical and radiological findings in six additional patients. *Cortex* **22**, 243-252 (1986).
52 De Schonen, S., De Diaz, M. G. & Mathivet, E. in *Aspects of face processing* 199-209 (Springer, 1986).
53 de Schonen, S. & Mathivet, E. Hemispheric asymmetry in a face discrimination task in infants. *Child Dev* **61**, 1192-1205 (1990).
54 Deruelle, C. & de Schonen, S. Do the right and left hemispheres attend to the same visuospatial information within a face in infancy? *Developmental Neuropsychology* **14**, 535-554 (1998).
55 Kostovic, I. & Jovanov-Milosevic, N. The development of cerebral connections during the first 20-45 weeks' gestation. *Semin Fetal Neonatal Med* **11**, 415-422, doi:10.1016/j.siny.2006.07.001 (2006).
56 Brody, B. A., Kinney, H. C., Kloman, A. S. & Gilles, F. H. Sequence of central nervous system myelination in human infancy. I. An autopsy study of myelination. *J Neuropathol Exp Neurol* **46**, 283-301 (1987).
57 Yakovlev PI, L. A. *The myelogenetic cycles of regional maturation in the brain.* . 3-69 (Oxford: Blackwell, 1967).
58 Nakagawa, H. *et al.* Normal myelination of anatomic nerve fiber bundles: MR analysis. *AJNR Am J Neuroradiol* **19**, 1129-1136 (1998).
59 Levitan, S. & Reggia, J. A. A computational model of lateralization and asymmetries in cortical maps. *Neural Comput* **12**, 2037-2062 (2000).
60 de Schonen, S. & Bry, I. Interhemispheric communication of visual learning: a developmental study in 3-6-month old infants. *Neuropsychologia* **25**, 601-612 (1987).
61 Liégeois, F., Bentejac, L. & de Schonen, S. When does inter-hemispheric integration of visual events emerge in infancy? A developmental study on 19-to 28-month-old infants. *Neuropsychologia* **38**, 1382-1389 (2000).
62 Sann, C. & Streri, A. Perception of object shape and texture in human newborns: evidence from cross-modal transfer tasks. *Dev Sci* **10**, 399-410, doi:10.1111/j.1467-7687.2007.00593.x (2007).
63 Flechsig, P. E. *Anatomie des menschlichen Gehirns und Rückenmarks auf myelogenetischer Grundlage*. Vol. 1 (G. Thieme, 1920).
64 Dubois, J. *et al.* The early development of brain white matter: a review of imaging studies in fetuses, newborns and infants. *Neuroscience* **276**, 48-71, doi:10.1016/j.neuroscience.2013.12.044 (2014).
65 Neil, J., Miller, J., Mukherjee, P. & Huppi, P. S. Diffusion tensor imaging of normal and injured developing human brain - a technical review. *NMR Biomed* **15**, 543-552, doi:10.1002/nbm.784 (2002).
66 Song, S. K. *et al.* Diffusion tensor imaging detects and differentiates axon and myelin degeneration in mouse optic nerve after retinal ischemia. *Neuroimage* **20**, 1714-1722 (2003).
67 Song, S. K. *et al.* Demyelination increases radial diffusivity in corpus callosum of mouse brain. *Neuroimage* **26**, 132-140, doi:10.1016/j.neuroimage.2005.01.028 (2005).

68 McCulloch, D. L., Orbach, H. & Skarf, B. Maturation of the pattern-reversal VEP in human infants: a theoretical framework. *Vision Res* **39**, 3673-3680 (1999).
69 Westerhausen, R. *et al.* Interhemispheric transfer time and structural properties of the corpus callosum. *Neurosci Lett* **409**, 140-145, doi:10.1016/j.neulet.2006.09.028 (2006).
70 Whitford, T. J. *et al.* Predicting inter-hemispheric transfer time from the diffusion properties of the corpus callosum in healthy individuals and schizophrenia patients: a combined ERP and DTI study. *Neuroimage* **54**, 2318-2329, doi:10.1016/j.neuroimage.2010.10.048 (2011).
71 Horowitz, A. *et al.* In vivo correlation between axon diameter and conduction velocity in the human brain. *Brain Struct Funct* **220**, 1777-1788, doi:10.1007/s00429-014-0871-0 (2015).
72 Akaike, H. in *International Encyclopedia of Statistical Science* 25-25 (Springer, 2011).
73 Lippe, S., Roy, M. S., Perchet, C. & Lassonde, M. Electrophysiological markers of visuocortical development. *Cereb Cortex* **17**, 100-107, doi:10.1093/cercor/bhj130 (2007).
74 Allen, D., Tyler, C. W. & Norcia, A. M. Development of grating acuity and contrast sensitivity in the central and peripheral visual field of the human infant. *Vision Res* **36**, 1945-1953 (1996).
75 Tachibanaki, S., Arinobu, D., Shimauchi-Matsukawa, Y., Tsushima, S. & Kawamura, S. Highly effective phosphorylation by G protein-coupled receptor kinase 7 of light-activated visual pigment in cones. *Proc Natl Acad Sci U S A* **102**, 9329-9334, doi:10.1073/pnas.0501875102 (2005).
76 Saron, C. D. & Davidson, R. J. Visual evoked potential measures of interhemispheric transfer time in humans. *Behav Neurosci* **103**, 1115-1138 (1989).
77 Honda, Y., Watanabe, S., Nakamura, M., Miki, K. & Kakigi, R. Interhemispheric difference for upright and inverted face perception in humans: an event-related potential study. *Brain Topogr* **20**, 31-39, doi:10.1007/s10548-007-0028-z (2007).
78 Ringo, J. L., Doty, R. W., Demeter, S. & Simard, P. Y. Time is of the essence: a conjecture that hemispheric specialization arises from interhemispheric conduction delay. *Cereb Cortex* **4**, 331-343 (1994).
79 Kulke, L., Atkinson, J. & Braddick, O. Automatic Detection of Attention Shifts in Infancy: Eye Tracking in the Fixation Shift Paradigm. *PLoS One* **10**, e0142505, doi:10.1371/journal.pone.0142505 (2015).
80 Rossion, B. & Caharel, S. ERP evidence for the speed of face categorization in the human brain: Disentangling the contribution of low-level visual cues from face perception. *Vision Res* **51**, 1297-1311, doi:10.1016/j.visres.2011.04.003 (2011).
81 Yovel, G., Tambini, A. & Brandman, T. The asymmetry of the fusiform face area is a stable individual characteristic that underlies the left-visual-field superiority for faces. *Neuropsychologia* **46**, 3061-3068, doi:10.1016/j.neuropsychologia.2008.06.017 (2008).
82 Kobayashi, M., Cassia, V. M., Kanazawa, S., Yamaguchi, M. K. & Kakigi, R. Perceptual narrowing towards adult faces is a cross-cultural phenomenon in infancy a behavioral and near-infrared spectroscopy study with Japanese infants, Developmental Science Early View. *Developmental Science*, n/a (2016).
83 Kobayashi, M. *et al.* Do infants represent the face in a viewpoint-invariant manner? Neural adaptation study as measured by near-infrared spectroscopy. *Front Hum Neurosci* **5**, 153, doi:10.3389/fnhum.2011.00153 (2011).
84 Sangrigoli, S. & De Schonen, S. Recognition of own-race and other-race faces by three-month-old infants. *J Child Psychol Psychiatry* **45**, 1219-1227, doi:10.1111/j.1469-7610.2004.00319.x (2004).
85 Bhatt, R. S., Bertin, E., Hayden, A. & Reed, A. Face processing in infancy: developmental changes in the use of different kinds of relational information. *Child Dev* **76**, 169-181, doi:10.1111/j.1467-8624.2005.00837.x (2005).
86 Bhatt, R. S., Bertin, E., Hayden, A. & Reed, A. Face Processing in Infancy Developmental Changes in the Use of Different Kinds of Relational Information, Child Development Volume 76, Issue 1. *Child Development* **76**, 169-181 (2005).
87 Weiner, K. S. *et al.* The Cytoarchitecture of Domain-specific Regions in Human High-level Visual Cortex. *Cereb Cortex*, doi:10.1093/cercor/bhw361 (2016).

88 Kabdebon, C. *et al.* Anatomical correlations of the international 10-20 sensor placement system in infants. *Neuroimage* **99**, 342-356, doi:10.1016/j.neuroimage.2014.05.046 (2014).
89 Dubois, J. *et al.* Correction strategy for diffusion-weighted images corrupted with motion: application to the DTI evaluation of infants' white matter. *Magn Reson Imaging* **32**, 981-992, doi:10.1016/j.mri.2014.05.007 (2014).
90 Duclap D., L. A., Schmitt B. ,Riff O., Guevara P. , Marrakchi-Kacem L. , Brion V. , Poupon F. , Mangin J.-F. , and Poupon C. . in *29th ESMRMB.*
91 Behrens, T. E., Berg, H. J., Jbabdi, S., Rushworth, M. F. & Woolrich, M. W. Probabilistic diffusion tractography with multiple fibre orientations: What can we gain? *Neuroimage* **34**, 144-155, doi:10.1016/j.neuroimage.2006.09.018 (2007).
92 Hua, K. *et al.* Tract probability maps in stereotaxic spaces: analyses of white matter anatomy and tract-specific quantification. *Neuroimage* **39**, 336-347, doi:10.1016/j.neuroimage.2007.07.053 (2008).
93 Delorme, A. & Makeig, S. EEGLAB: an open source toolbox for analysis of single-trial EEG dynamics including independent component analysis. *J Neurosci Methods* **134**, 9-21, doi:10.1016/j.jneumeth.2003.10.009 (2004).
94 Tadel, F., Baillet, S., Mosher, J. C., Pantazis, D. & Leahy, R. M. Brainstorm: a user-friendly application for MEG/EEG analysis. *Comput Intell Neurosci* **2011**, 879716, doi:10.1155/2011/879716 (2011).
95 Kouider, S. *et al.* A neural marker of perceptual consciousness in infants. *Science* **340**, 376-380, doi:10.1126/science.1232509 (2013).

Acknowledgements:

This research was supported by grants from the Fondation de France and the Fyssen Foundation. The funders had no role in study design, data collection and analysis, decision to publish, or preparation of the manuscript. The authors would like to thank all the infants and their parents who participated in this study as well as Giovanna Santoro and the medical team of UNIACT at Neurospin, who helped in carrying out the experiments. We are also grateful to Claire Kabdebon, Pablo Barttfeld, Jessica Lebenberg and Francois Leroy for their help in EEG and MRI analyses, and Eric Moulton for proofreading the text.

Authors Contribution:

All authors contributed to data collection, analysis, interpretation as well as drafting the article. J.D. and G.D.L. designed the experiments.

Competing interests statement:

The authors declare no competing interests.

Figures:

Figure 1: EEG experimental paradigms

a) Centralized presentation: A stream of female (or male) face images was presented at the center of the screen. Each face was presented during 250 ms, separated by a random interval of 550 to 950 ms during which a rotating and colored bull's-eye was presented at the center of the screen.

b) Lateralized presentation: Two streams of face images were presented in the left and right visual hemifields in an alternating fashion. The colored bull's-eye was always rotating at the center of the screen to attract the infants' gaze toward the center of the screen and to avoid saccades to the periphery. In each block of the experimental design, one face image was attributed to each side and was presented for 250 ms followed by a post-stimulus random interval of 550 to 950 ms. Each block consisted of only female or only male images.

c) The different conditions of the lateralized paradigm: For each block, one standard face was attributed to one side and presented in ~ 80% of trials. In ~ 10% of trials, known-deviant faces corresponded to the standard faces on the incorrect side whereas new deviant faces were rare faces with no attributed side (~ 10% of trials). For copyright reasons, the right standard face is different from the one presented in the experiment.

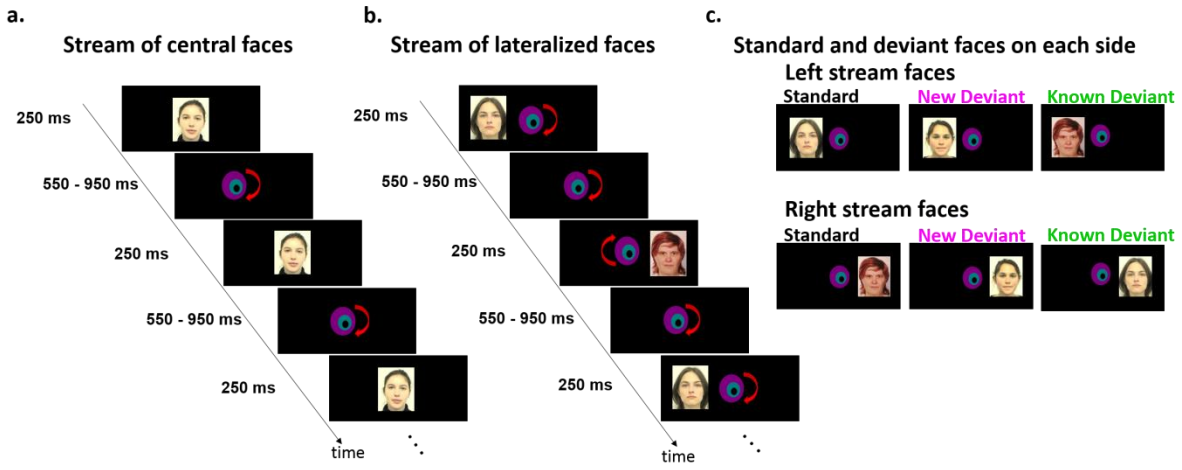

Figure 2. P1 component

a) Voltage time course in response to central stimuli averaged over a cluster of electrodes covering the mid-occipital region in one infant (21 weeks old). Time zero marks the onset of the face stimuli.

b) Responses to faces presented in the right hemifield averaged across the left and right occipital clusters of electrodes (red and blue curves respectively) in the same infant. The contralateral P1 appears over the left hemisphere and then propagates toward the ipsilateral hemisphere.

c) Relation between P1 latencies and age over the infants group: P1 for central stimuli (black curve, 23 infants), contralateral P1 for lateralized stimuli (red curve, 40 infants), and inter-hemispheric transfer-time (blue curve, 40 infants). P1 latencies were faster for central than for lateralized stimuli and reached a plateau after 12 weeks of age, whereas the decrease was linear for the contralateral P1 and the inter-hemispheric transfer times.

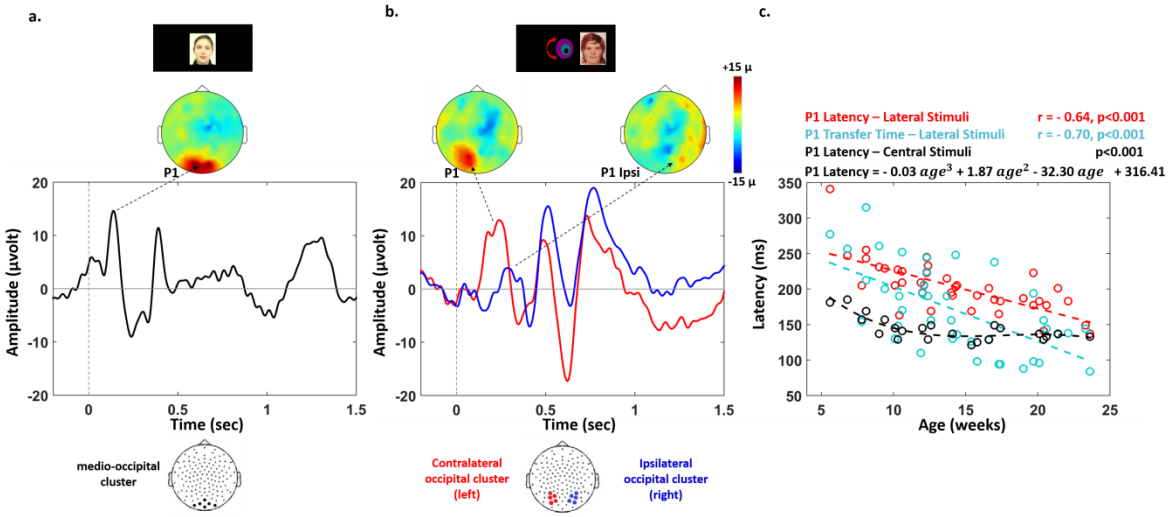

Figure 3: Structure-function relationships

a) Reconstructed bundles of the visual network in one infant (12 weeks old): optic radiations, extending from the lateral geniculate nucleus to occipital regions (top), and callosal fibers connecting the occipital regions and passing through the splenium (bottom).

b) Age-related decrease of transverse diffusivity in optic radiations (red) and visual callosal fibers (blue) in the 22 infants with MRI data.

c) Age-related increase of response speeds (speed ~ anatomical distance/latency) corresponding to P1 (red) and IHTT (blue) responses in the 13 infants with both EEG and MRI data.

d) Relationships between the response speed and transverse diffusivity ($\lambda_\perp$) in the corresponding tract for the 13 infants with EEG and MRI data. Partial correlations were performed to demonstrate that speeds are related to diffusivities, independently of age. To visualize such relationships, we here show the residuals once the effect of age was removed, for P1 (left) and IHTT (right) speeds in relation to $\lambda_\perp$ in the optic radiations (left) and visual callosal fibers (right). r and p values correspond to partial correlations reported in the text and Table 1.

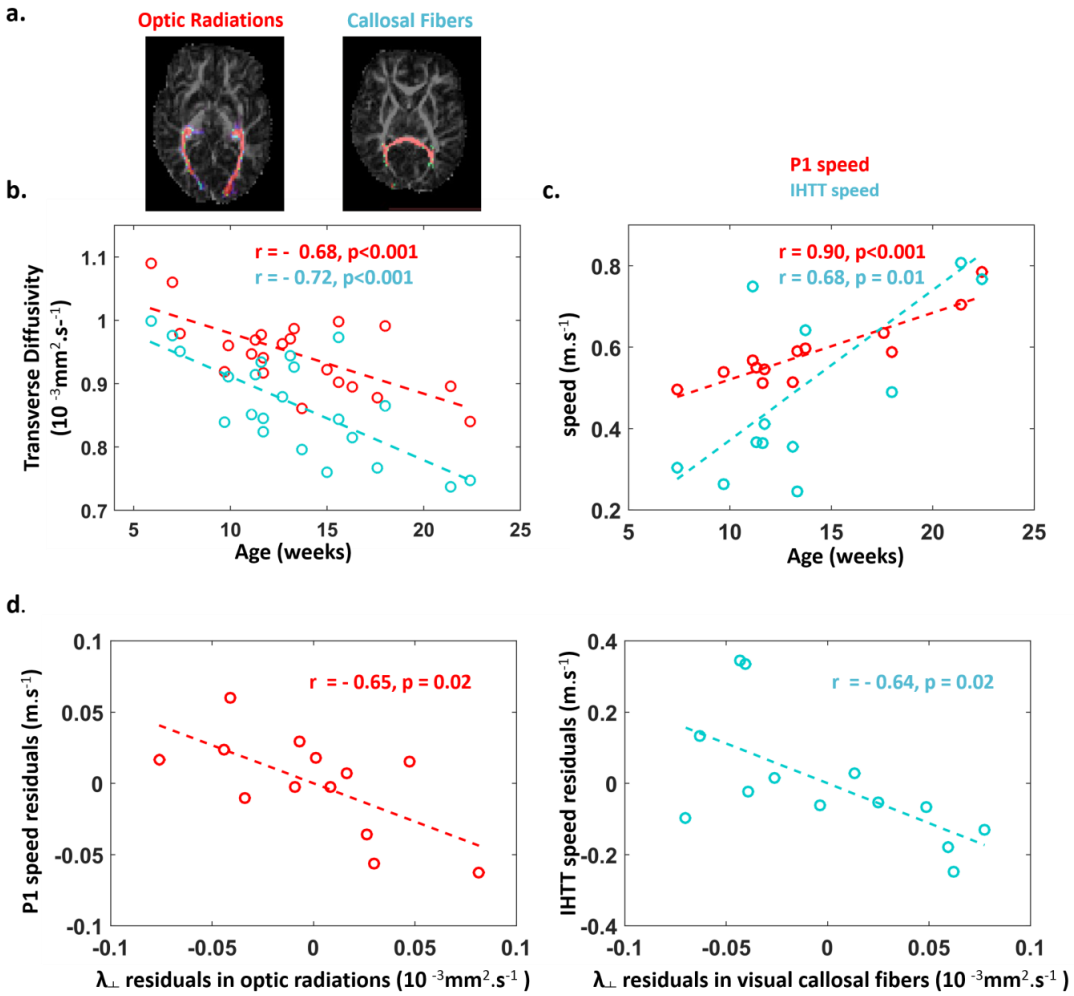

Figure 4: Grand averages according to the visual hemifields

Top row) Grand-averages of the 40 infants were computed over the left (red line) and right (blue line) occipito-temporal clusters presented below the plots, for faces presented in the left and right visual hemifields. The peaks of the N290 and P400 are indicated on the plots. Bottom row) 2D voltage topographies. The N290 interrupts the positivity on the contra-lateral cluster and the ascending slope on the ipsi-lateral cluster. We consider the following positivity as the P400. Latencies are delayed relative to what is reported for central faces.

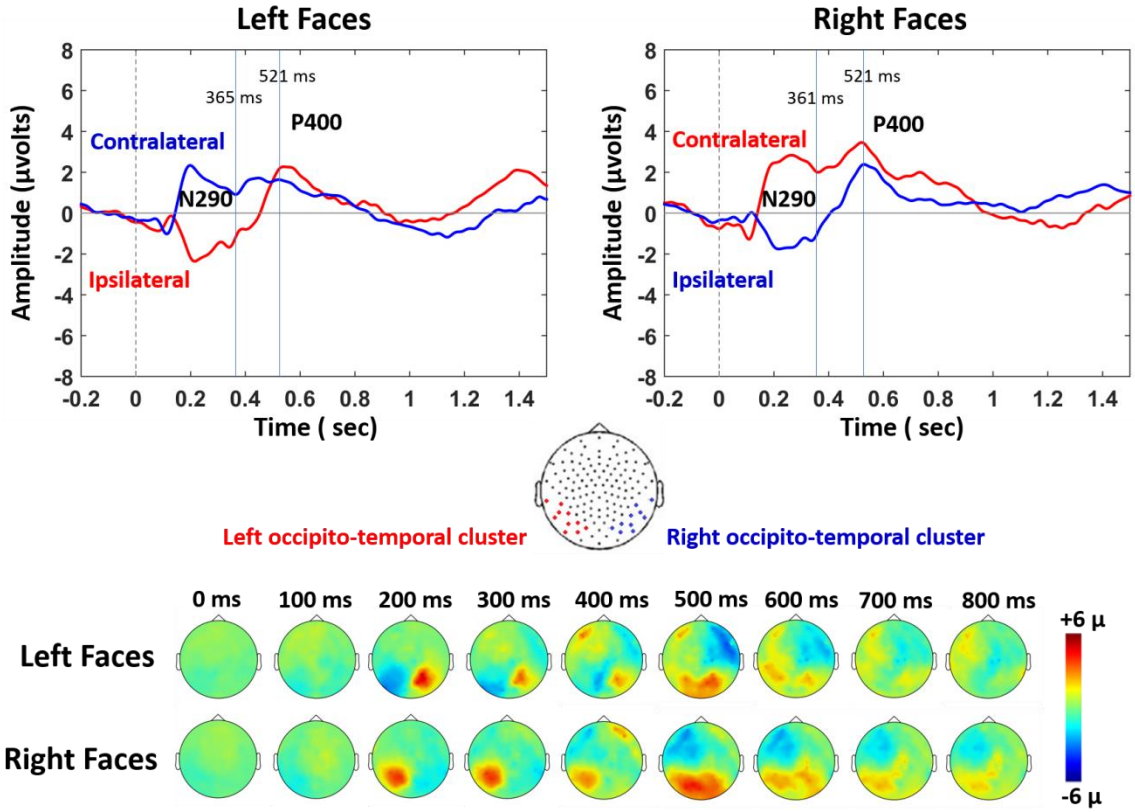

Figure 5: Grand averages according to the face conditions

Grand-averages of the 40 infants were computed over the left and right occipito-temporal clusters (left and right plots respectively) for the new-deviant, known-deviant and standard faces presented in the left (a) and right (b) visual hemifields. Shaded regions around ERPs represent standard mean error of the mean. Voltage topographies (right column) were averaged over the [300-400] ms and [450-550] ms time-windows (shaded in light blue in the time plots) corresponding to the N290 and P400 respectively (note that voltage topographies for other time windows along the trials are presented in supplementary information). There is a clear discrimination of new faces relative to the standard and known-deviant faces for the left hemifield faces over the contra-lateral right cluster, whereas no difference between conditions was observed for the right hemifield faces.

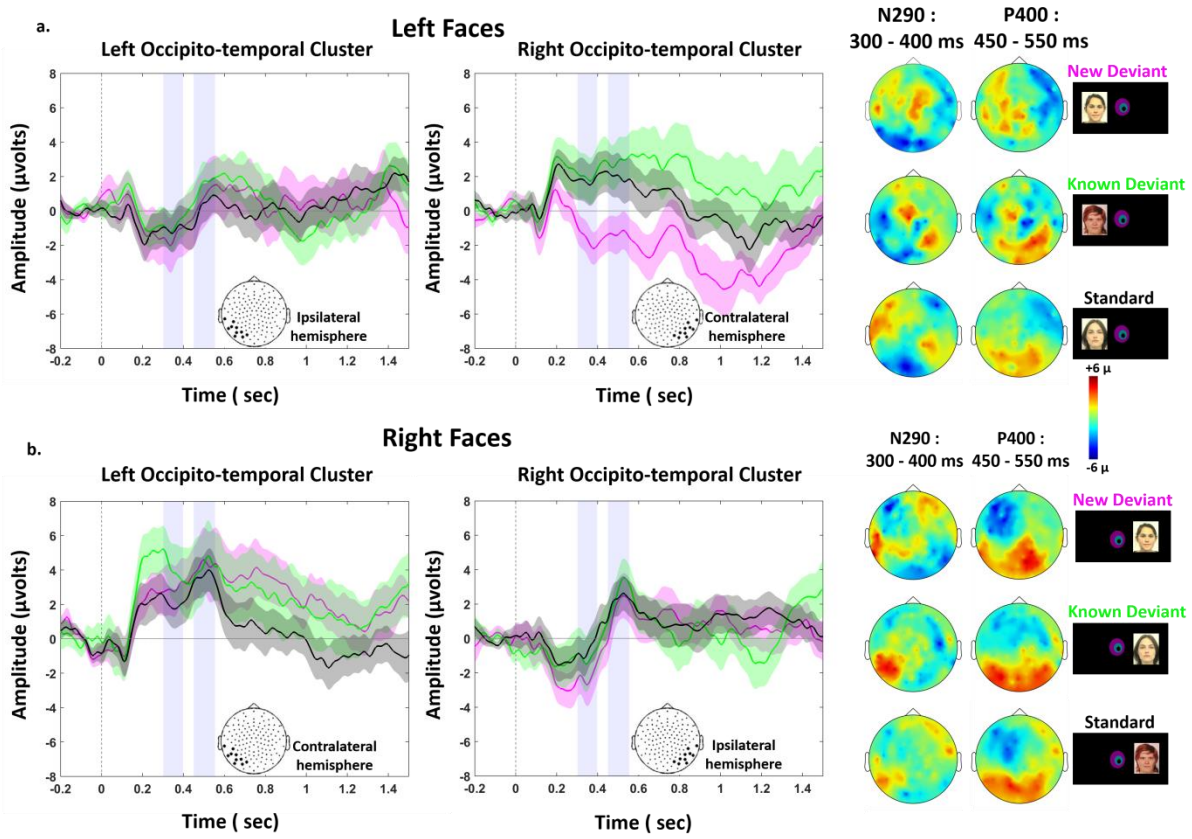

Figure 6: Comparison of N290 and P400 components across face conditions

N290 (upper row) and P400 (lower row) amplitudes for faces presented in the left (a) and right (b) hemifield averaged over the left and right clusters (left and right plots respectively) in the different face conditions (new-deviant faces in pink, known-deviant faces in green, standard faces in black). The error bars represent the standard mean error across the 40 individuals. * highlights the significant differences between conditions after FDR correction for multiple comparisons ($p < 0.05$). In c) the differences between conditions for left hemifield faces averaged over the right cluster are plotted as a function of infants age. There was an increase of the discrimination ability for new-deviant vs standard faces (a significant decrease of N290 amplitude and a non-significant trend for P400 in the left plots) but not vs know-deviant faces (right plots, n.s. non-significant $p > 0.1$).

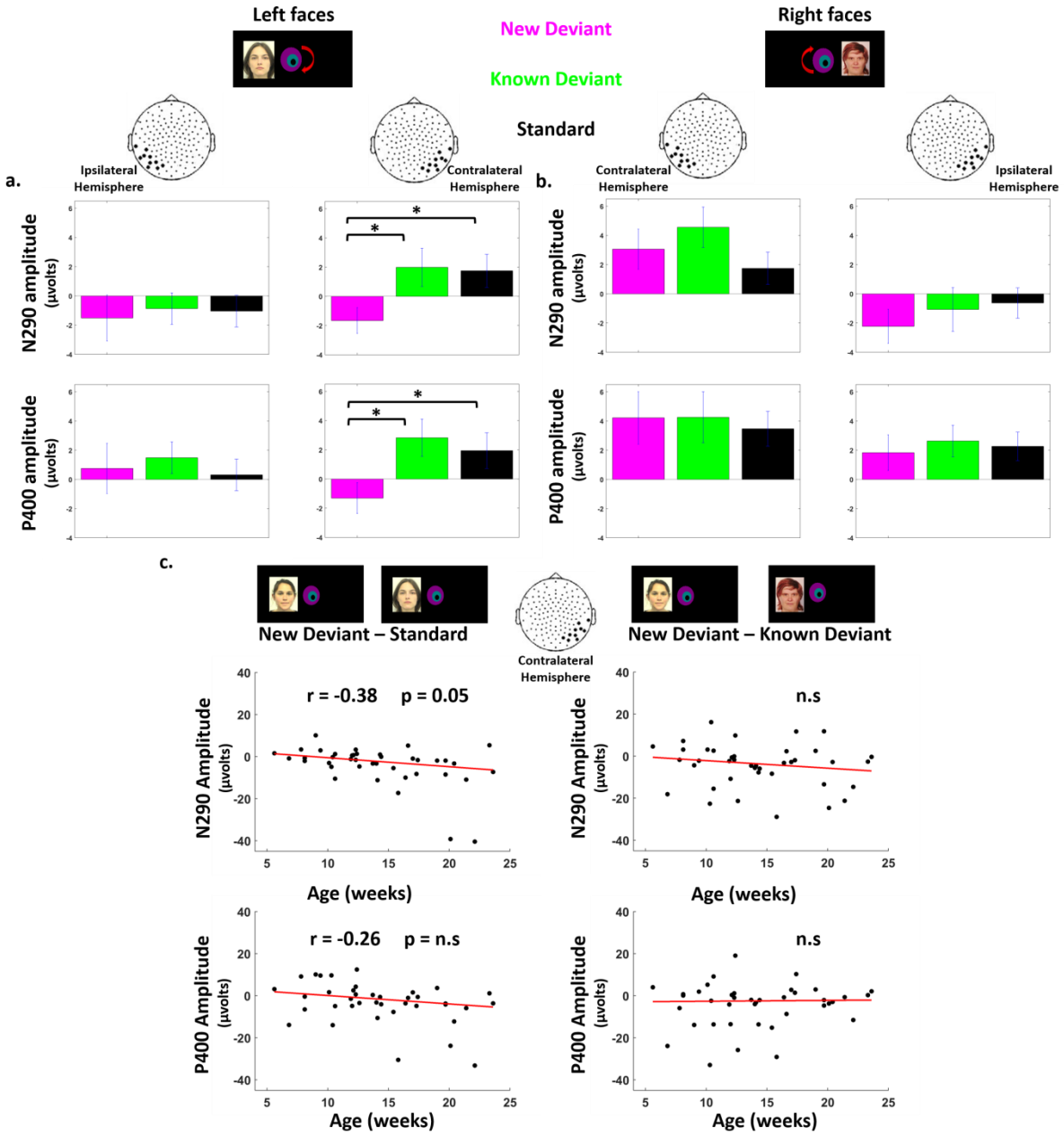

Tables:

Table 1: Evaluation of structural maturation with DTI

Left panel: partial correlations were computed for transverse diffusivity in the different pairs of bundles, while controlling for the infants age. Optic and acoustic radiations, visual and auditory callosal fibers are abbreviated by OR, AR, vCC and aCC, respectively. Right panel: partial correlations were computed between the speed of P1 or IHTT and transverse diffusivity in similar bundles of the visual and auditory networks, while controlling for age. P values are corrected for the number of comparisons with FDR approach.

Maturational relationships across bundles				Structure-function relationships		
	vCC	**AR**	**aCC**		**Speed P1**	**Speed IHTT**
OR	r = 0.78, p < 0.001	r = 0.63, p = 0.004	r = 0.55, p = 0.014	**OR**	r = - 0.65, p = 0.021	
vCC		r = 0.35, p > 0.1	r = 0.74, p < 0.001	**vCC**		r = - 0.64, p = 0.025
AR			r = 0.42, p = 0.069	**AR**	r = - 0.45, p > 0.1	
aCC				**aCC**		r = - 0.65, p = 0.021

Table 2: Comparison of P1, N290 and P400 responses for the different face conditions

The effect of face condition was tested using separate ANOVAs for different ERP components (P1, N290 and P400 responses) and for faces presented in the left (a) and right (b) hemifield. The main effects of experimental condition are reported before post-hoc t-tests analyses. P values are corrected for multiple comparisons using FDR approach.

Left Faces		
	Left occipito-temporal cluster	**Right occipito-temporal cluster**
P1	F = 0.2 , p > 0.1	F = 2.4 , p = 0.101
N290	F = 0.1 , p > 0.1	F = 5.1 , p = 0.016 New vs. Standard: t = -2.7 , p = 0.014 Known vs. Standard: t = 0.2 , p > 0.1 New vs. Known: t = -2.7 , p = 0.014
P400	F = 0.2 , p > 0.1	F = 3.9 , p = 0.047 New vs. Standard: t = -2.3 , p = 0. 042 Known vs. Standard: t = 0.5 , p > 0.1 New vs. Known: t = -2.7 , p = 0.029
Right Faces		
	Left occipito-temporal cluster	**Right occipito-temporal cluster**
P1	F =2.5, p = 0.090 New vs. Standard: t = 0.1 , p > 0.1 Known vs. Standard: t = 2.5 , p = 0.042 New vs. Known: t = -1.7 , p > 0.1	F = 0.5 , p > 0.1
N290	F = 1.5 , p > 0.1	F = 0.6 , p > 0.1
P400	F = 0.1 , p > 0.1	F = 0.2 , p > 0.1

Supplementary Figure: 2D topographies of the grand averages in the different conditions

The top and bottom rows correspond to the left- and right- hemifield presentation of faces respectively. The early response is clearly contra-lateralized relative to the visual stimulation, then becomes more bilateral due to inter-hemispheric transfer. For the new-deviant left faces, there is a decrease in the activity over occipito-temporal areas from ~300 onwards, referring to the discrimination responses. The time course of activity over occipito-temporal areas are represented in figure 5.